

# Local semiconducting transition in armchair carbon nanotubes: The effect of periodic bi-site perturbation on electronic and transport properties of carbon nanotubes

M. J. Hashemi, K. Sääskilähti, and M. J. Puska

*Department of Applied Physics, Aalto University, P.O. Box 11100, FI-00076 Aalto, Finland*

(Received 28 October 2010; published 10 March 2011)

In carbon nanotubes, the most abundant defects, caused for example by irradiation or chemisorption treatments, are small perturbing clusters, i.e., bi-site defects, extending over both A and B sites. The relative positions of these perturbing clusters play a crucial role in determining the electronic properties of carbon nanotubes. Using band structure and electronic transport calculations, we find that in the case of armchair metallic nanotubes a band gap opens up when the clusters fulfill a certain periodicity condition. This phenomenon might be used in future nanoelectronic devices in which certain regions of single metallic nanotubes could be turned to semiconducting ones. Although in this work we study specifically the effect of hydrogen adatom clusters, the phenomenon is general for different types of defects. Moreover, we study the influence of the length and randomness of the defected region on the electron transport through it.

DOI: [10.1103/PhysRevB.83.115411](https://doi.org/10.1103/PhysRevB.83.115411)

PACS number(s): 73.63.Fg, 72.10.Fk

## I. INTRODUCTION

Carbon based materials, carbon nanotubes and graphene, are considered as the most promising candidates for many future technological applications because of their unique electronic, mechanical, and optical properties.<sup>1</sup> In the case of single wall carbon nanotubes (SWCNTs), the chirality and diameter determine whether a SWCNT is metallic or semiconducting.<sup>2</sup> In particular, armchair nanotubes with the  $(n,n)$ -type chiral vectors are metallic, enabling their use as ultimate leads in nanoelectronics.

Assuming the possibility of chirality-sensitive selection of nanotubes the first step toward single-SWCNT nanoelectronic devices is the formation of rectifying metal-semiconductor junctions. Occasionally, these kinds of junctions are realized due to pentagon-heptagon defects making a seamless junction between nanotubes of different chiralities.<sup>3,4</sup> More intentionally, nanotubes of different character can also be electron-beam welded at elevated temperatures to form X, T, and Y junctions.<sup>5</sup> Moreover, recently Lee *et al.*<sup>6</sup> suggested the joining of different types of nanotubes with covalent peptide linkages. Another route is to modify the electronic band structure of a single SWCNT spatially by functionalization with defects, adatoms, or molecules, or by controlled deformation. The use of modulating (saturation) hydrogen adsorption<sup>7</sup> or radial deformation<sup>8</sup> has been suggested to create quantum well structures for charge carriers. As a potential method, Wall and Ferreira<sup>9</sup> modeled also the effects of helical wrapping of polymeric molecules around SWCNTs.

Imperfections and their causes and effects in SWCNTs have been the subject of detailed studies for a long time.<sup>10–13</sup> For instance, pointlike vacancies, defects, and adsorbed atoms are known as a source of reduction in electronic transmission through nanotubes.<sup>14–19</sup> The carbon atoms of a nanotube belong to two sublattices, A and B, and then in the case of more than one adsorbate the effect on the transmission strongly depends on whether the adsorbates are on the same sublattice, A or B, or on different ones, A and B, as well as on their relative positions.<sup>16,19,20</sup> In a recent study, García-Lastra *et al.*<sup>20</sup> showed that the relative position dependence obeys a certain

rule if the adsorbates are on the same sublattice, while they did not find any trend for adsorbates on different sublattices. Considering the difficulty of realizing such site-selective perturbations and the abundance of extended bi-site perturbations in experiments, it is also important to understand how defect clusters (collectively) affect the electronic properties of carbon nanotubes.

In this paper we discuss the effect of perturbing defect clusters spanning both the A and B sublattices and we refer to them as bi-site perturbances or bi-site defects. In particular we discuss how undoped armchair SWCNTs can locally be turned from metallic to semiconducting by periodic bi-site perturbations. We study the effects of repeated small hydrogen clusters (Fig. 1) on SWCNTs, but our main qualitative results are valid also for arbitrary bi-site perturbation. We discuss how the electron transport through armchair SWCNTs is affected by bi-site perturbations of different number, strength, and periodicity along the SWCNT. Our calculations for the metallic armchair SWCNTs show that when a certain rule for the relative positions of the defect clusters is fulfilled, an energy gap around the Fermi level opens gradually by increasing the length of the periodically defected region. We study the robustness of this effect against randomness in cluster size and geometry as well as in the clusters' relative positions. Hydrogen clusters are realistic defect candidates because calculations and experiments show that adsorbed hydrogen atoms tend to cluster on SWCNTs' sidewalls.<sup>21–23</sup> The rapid development in pattern making, e.g., using block copolymer nanolithography,<sup>24,25</sup> and in fine-tuning and manipulating structures even on the angstrom scale<sup>26</sup> may make regular defect systems feasible and relevant also in the experimental and practical sense.

The organization of the present article is as follows. In Sec. II we present the systems studied and their notation as well as the methods used in electronic structure and transport calculations. Section III comprises our results and discussion. Section IV is a short summary.

## II. SYSTEMS AND METHODOLOGY

First we perform a set of supercell band structure calculations in which supercells consist of a certain number of

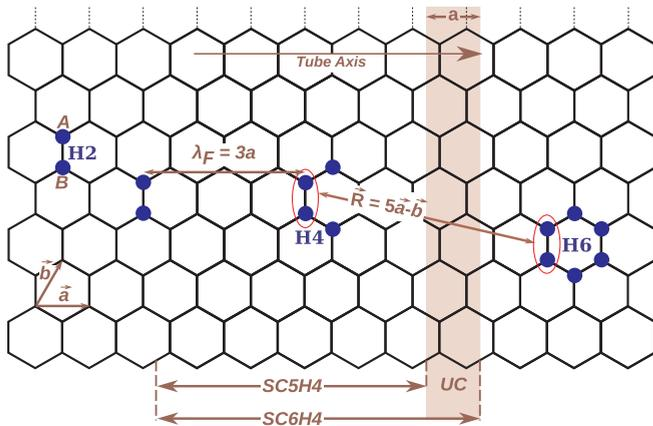


FIG. 1. (Color online) Three different hydrogen clusters—H2, H4, and H6 (blue circles)—used in the calculations. They are shown on a piece of an armchair SWCNT’s surface. The unit vectors of the graphene sheet ( $\vec{a}$  and  $\vec{b}$ ), the A and B sublattices, the Fermi wavelength ( $\lambda_F = 3a$ ), and a vector connecting the adjacent hydrogen clusters are also given. The unit cell (UC) of the pristine tube with the length “ $a$ ,” as well as superlattice unit cells corresponding to two different periodicities of the hydrogenated SWCNTs (SC5H4 and SC6H4), are shown.

unit cells of a pristine armchair SWCNT and four hydrogen atoms adsorbed on neighboring carbon atoms, as shown in Fig. 1. In particular, we choose the (8,8) nanotube which has a diameter close to that often seen in experiments. We adopt, for example, the notation SC5H4 for the supercell comprising five (8,8) SWCNT unitcells (SC5) and an adsorbed cluster of four hydrogen atoms (H4), as depicted in Fig. 1. The essential criterion for these clusters is that they have to perturb both the A and B sublattices in a plane perpendicular to the tube axis. Similar clusters with an odd number of hydrogen atoms would lead to similar effects. Because we are interested in the main qualitative results and want to avoid complications due to spin effects, we neglect these odd-atom clusters in our studies.

The electronic structures are solved with density functional theory (DFT) within the PBE generalized gradient approximation<sup>27</sup> for electron exchange and correlation. We employ the SIESTA package<sup>28</sup> with nonlocal norm-conserving pseudopotentials<sup>29</sup> and a double-zeta plus polarization (DZP) atomic orbital basis set. The atomic geometry and the supercell size are relaxed until all atomic forces are less than 0.02 eV/Å. C-C and C-H bond lengths in close agreement with experiments are obtained.

Thereafter structures for the transport calculations are made of two semi-infinite pristine (8,8) SWCNT leads and a central region with a varying content. In order to see how prolongation of the periodically defected region changes the influence of hydrogen clusters on the electronic transport of nanotubes, we consider central regions consisting of varying numbers of the different, above-mentioned supercells. For example, we may have ten SC5H4 supercells, and we denote this as the 10(SC5H4) scattering region. Finally, we have at each end of the central region a unit cell of the (8,8) SWCNT nanotube to ensure nonreflecting semi-infinite leads.

Our transport calculations are done using the Landauer-Büttiker formalism. We construct the Hamiltonian matrix

using the tight-binding method with nearest-neighbor hopping. Because carbon atoms take part in the transport process by the  $p_z$  orbitals, the carbon atoms using them in bonding with on-top adsorbed hydrogen atoms will not participate in the transport process anymore. In our tight-binding transport calculations, we simulate this effect by removing the host carbon atoms binding to hydrogen atoms. For benchmarking we compare the transmission functions of a single SC6H4 supercell obtained by the tight-binding method with that calculated by the DFT Transiesta program.<sup>30</sup> When the hopping parameter  $t$  has a value of 2.3 eV we find a very good agreement particularly around the Fermi level (see the lower left panel of Fig. 3).

### III. RESULTS AND DISCUSSION

Figure 2 shows our DFT results for the band structures of the pristine (8,8) SWCNT as well as those of (8,8) nanotubes decorated periodically with H4 clusters. The band structures are shown with increasing supercell length; i.e., they correspond to the SC1H0, SC4H4, SC5H4, and SC6H4 supercells. The increase of the supercell length folds the band structure of the pristine single-unit-cell nanotube as shown by dotted lines in Figs. 2(b)–2(d). There are qualitatively two different repeating band structure schemes with respect to the band crossing point at the Fermi energy represented by the SC4H4 or SC5H4 supercells and the SC6H4 supercell. The band structures of the H-cluster decorated nanotubes with different supercell lengths follow roughly those of the pristine nanotube. However, there is an important qualitative difference. In the case of the SC6H4 supercell a band gap

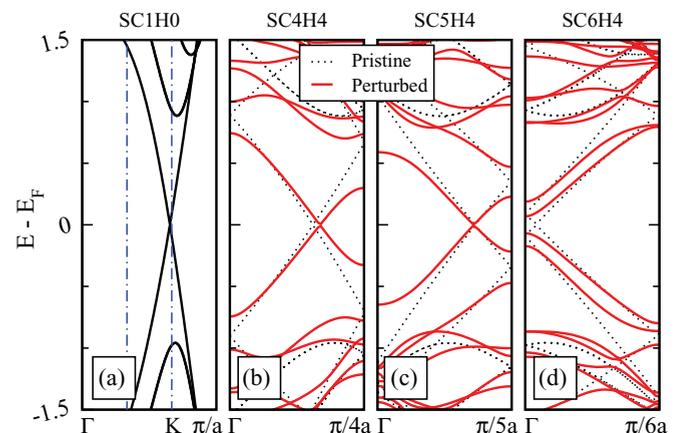


FIG. 2. (Color online) Effect of the periodically repeated H4 clusters on the band structure of the (8,8) SWCNT. The band structure of (a) the pristine nanotube SC1H0 is compared to those for nanotubes with H-atom clusters and different supercell lengths, i.e., for (b) SC4H4, (c) SC5H4, and (d) SC6H4 (for the notation see the text and Fig. 1). “ $a$ ,” on the wave vector axis, is the length of the CNT unit cell, as shown in Fig. 1. The dotted lines in (b)–(d) denote the band structure of the pristine nanotube folded according to the length of the supercell. The (blue) dashed lines in panel (a) are band or Brillouin zone folding lines for SC3H0. For any SC(3M) with an integer  $M$ , these lines are two of the  $3M - 1$  folding lines. Therefore in all of these cases, the Fermi point is placed, after the folding, near the  $\Gamma$  point.

opens around the Fermi energy. The size of the band gap increases with the strength of the perturbation, e.g., as the number of the hydrogen atoms in the cluster increases. Further calculations with supercells containing several H-atom clusters show that such a band gap opening happens for all supercells in which the relative positions of the adjacent adsorbate clusters, or more generally bi-site perturbations, fulfill the condition

$$\vec{R} = p\vec{a} + q\vec{b}, \quad p - q = 3M, \quad |M \in \mathbb{Z}, \quad (1)$$

where  $\vec{a}$  and  $\vec{b}$  are the unit vectors given in Fig. 1. Thus, the clusters may be in different positions on the planes perpendicular to the tube axis as, for example, the different clusters in Fig. 1. Equation (1) is actually the condition that a pristine nanotube is metallic.<sup>2</sup> Moreover, it was found by García-Lastra *et al.*<sup>20</sup> to give also the rule that two molecules adsorbed on same sublattice sites of a SWNT leave one of the two transmission channels unaffected.

The above-mentioned metal to semiconductor transition can be understood as follows. When the length of the unit cell of a pristine armchair SWNT is artificially tripled the energy band crossing point at the Fermi level (corresponding to a  $K$  point in the first Brillouin zone of graphene) is folded close to the  $\Gamma$  point [see Fig. 2(a) for Brillouin zone folding lines]. Therefore, perturbations with this periodicity affect the band structure in the same way as the lattice potential in the nearly free electron model and open up a band gap around the Fermi level. The same happens for any periodicity length of  $3M$  times the unit cell length and also when the condition of Eq. (1) is fulfilled. But for the periodicity lengths of  $3M + 1$  or  $3M + 2$  times the unit cell length the band crossing point does not coincide with a reciprocal lattice boundary and the armchair SWNT remains metallic even with the bi-site perturbations.

To get another viewpoint on the origin of the band gap opening for certain periodic perturbations and to see how periodic bi-site perturbations of finite lengths affect

the transmission of the armchair SWCNT, we calculate the transmission functions of several nanotubes with a varying number of perturbed supercells in the central region. With increasing number of atoms, the use of DFT for transport calculations becomes prohibitively cpu-time consuming and therefore we employ a simple tight-binding method benchmarked against the DFT results. The upper and lower panels of Fig. 3 show the transmission functions for the  $N(\text{SC5H4})$  and  $N(\text{SC6H4})$  central region systems, respectively. The lengths of the periodic regions increase from left to right with  $N = 1, 2, 5,$  and  $10$ . It can be clearly seen that the transmission in the  $N(\text{SC6H4})$  systems decays and sharpens in the shape around the Fermi energy with the length of the periodically perturbed region.

In contrast, for the  $N(\text{SC5H4})$  systems, the transmission around the Fermi energy remains very close to that of the pristine armchair SWCNT and actually the several scatterings develop a nearly constant transmission plateau with the increasing length of the periodically perturbed region.

We plot in Fig. 4 the transmission coefficient at the Fermi energy for the  $N(\text{SC6H2})$ ,  $N(\text{SC6H4})$ , and  $N(\text{SC6H6})$  central region systems as a function of  $N$ . Although the stability of this H6 cluster has not been established in contrast to the H2 and H4 clusters,<sup>21</sup> we use the H6 cluster to qualitatively mimic the effect of stronger perturbations which cover a full hexagon. For long periodically perturbed regions, a nearly exponential decay can be seen in all three cases reflecting tunneling through a semiconducting region. In a natural manner, the decay rate increases strongly as a function of the cluster size.

We describe the above phenomena as follows. When the periodic perturbations occur with the separation of  $n\lambda_F/2$ , where  $n$  is an integer, all the backscattered electron waves at the Fermi level interfere constructively suppressing the transmission. As depicted in Fig. 1 the Fermi wavelength of an armchair SWCNT is  $3a$  and therefore the constructive interference of the backscattering waves takes place for

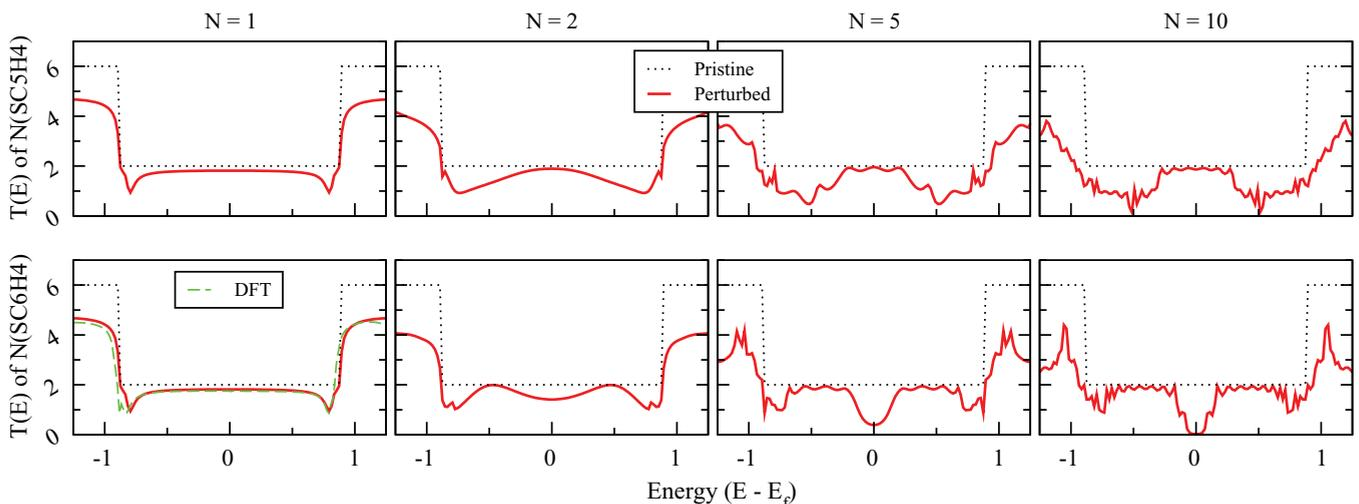


FIG. 3. (Color online) Effect of the relative positions and the number of bi-site perturbations on the transmission coefficient of armchair SWCNTs. The (red) solid curves in the upper and lower rows show the tight-binding results for central regions  $N(\text{SC5H4})$  and  $N(\text{SC6H4})$ , respectively. From left to right,  $N = 1, 2, 5,$  and  $10$ . The dotted black lines give the pristine transmission function. The dashed (green) curve in the lower left panel gives the DFT result calculated by the Transiesta program.

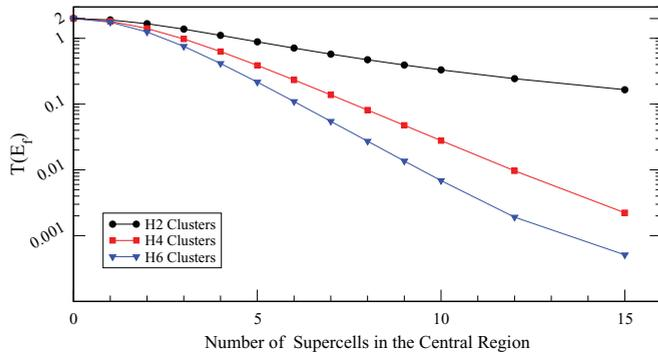


FIG. 4. (Color online) Fermi-energy transmission coefficient for  $N(\text{SC6H2})$ ,  $N(\text{SC6H4})$ , and  $N(\text{SC6H6})$  scattering regions as a function of  $N$ , the number of the perturbing supercells.

periodic central regions constructed, for example, from the SC6H4 supercells but not for those containing, for example, SC5H4 supercells (see Fig. 1).

Next, we explore with the tight-binding model the generality of our finding of the opening of the transmission gap at the Fermi level. We take the 10(SC6H4) central region system and change the positions of two of the H4 clusters so that they do not satisfy Eq. (1). Depending on which two of the clusters one chooses, the transmission changes, but not in a radical way. In all combinations the general trend of the decreasing transmission is conserved. In Fig. 5 the transmission at the Fermi level is shown for some of the combinations studied. The transmission is close to that of the 8(SC6H4) central region system when all the clusters satisfying Eq. (1) are adjacent to each others. When the clusters satisfying Eq. (1) are separated the transmission is close to that of the 7(SC6H4) central region system.

The effects of randomness in the size of the clusters as well as in their positions around the circumference perpendicular to the tube axis are also studied in the case of the 10(SC6H4) system. First we replace some of the H4 clusters with the H2 or H6 clusters and see that the transmission at the Fermi level stays low although the exact value depends on the particular combination in question. Next, in a set of separate calculations, we move the H4 clusters around the nanotube on the same perpendicular plane. We find that as long as the clusters fulfill Eq. (1), the same destructive effect on transmission occurs. Sample results labeled as *Different Clusters* and *Disaligned* are included in Fig. 5. Our findings show that the exact periodicity of the clusters is not playing the main role and the cluster species and their position around the tube may vary, for example, as depicted in Fig. 1.

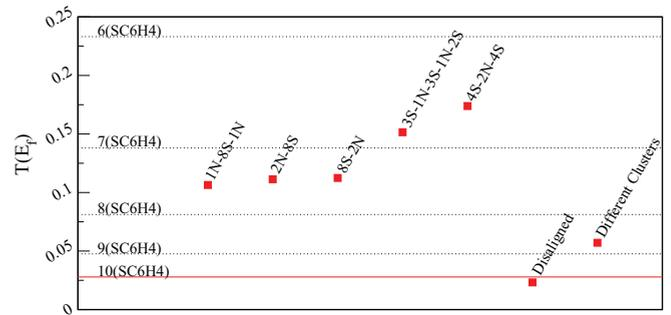


FIG. 5. (Color online) Fermi-energy transmission coefficient for different systems made by manipulating the original 10(SC6H4) system by displacing two of the H4 clusters. In the notation giving the sequence of the clusters, S and N stand for clusters *Satisfying* and *Not satisfying* the condition of Eq. (1). Sample results due to changing clusters' positions (*Disaligned*) around the circumference perpendicular to the tube axis and due to replacing some of the H4 clusters by H6 or H2 clusters (*Different Clusters*) are also shown. The solid (red) line is the Fermi-energy transmission value for the original 10(SC6H4) system and the (black) dotted lines are, for comparison, those for the  $N(\text{SC6H4})$  systems with  $N = 9, 8, 7$ , and 6.

Finally, we emphasize that our qualitative findings are valid regardless of the type of perturbations beyond the adsorbate clusters. For instance, our calculations for carbon nanobuds,<sup>31,32</sup> which can be viewed as an example of the perturbing a full hexagon, show exactly the same behavior. Moreover, according to our calculations also different hydrogenated vacancy clusters result in the same phenomenon.

#### IV. CONCLUSIONS

We have studied the effect of multiple bi-site perturbations on electronic and transport properties of armchair nanotubes. Our calculations show that following a certain relative-position condition, a naturally metallic nanotube can turn into semiconducting. The phenomenon shows robustness against variations in the types of perturbing species and also to some extent in their positions. The phenomenon is proposed as a means for creating single-SWCNT electronic devices.

#### ACKNOWLEDGMENTS

The work has been supported by the Finnish Academy through their Center of Excellence program. We are thankful to R. M. Nieminen, Ari Harju, and Maria Ganchenkova for useful discussions and A-P Jauho for his comments on the manuscript.

<sup>1</sup>M. Anantram and F. Léonard, *Rep. Prog. Phys.* **69**, 507 (2006).

<sup>2</sup>R. Saito, G. Dresselhaus, M. Dresselhaus *et al.*, *Physical Properties of Carbon Nanotubes* (Imperial College Press, London, 1999).

<sup>3</sup>R. F. Service, *Science* **271**, 1232 (1996).

<sup>4</sup>Z. Yao, H. W. C. Postma, L. Balents, and C. Dekker, *Nature (London)* **402**, 273 (1999).

<sup>5</sup>M. Terrones, H. Terrones, F. Banhart, J.-C. Charlier, and P. Ajayan, *Science* **288**, 1226 (2000).

<sup>6</sup>S. U. Lee, M. Khazaei, F. Pichierri, and Y. Kawazoe, *Phys. Chem. Chem. Phys.* **10**, 5225 (2008).

<sup>7</sup>O. Gülseren, T. Yildirim, and S. Ciraci, *Phys. Rev. B* **68**, 115419 (2003).

<sup>8</sup>C. Kilic, S. Ciraci, O. Gülseren, and T. Yildirim, *Phys. Rev. B* **62**, R16345 (2000).

<sup>9</sup>A. Wall and M. S. Ferreira, *J. Phys. Condens. Matter* **19**, 406227 (2007).

- <sup>10</sup>H. J. Choi, J. Ihm, S. G. Louie, and M. L. Cohen, *Phys. Rev. Lett.* **84**, 2917 (2000).
- <sup>11</sup>M. Igami, T. Nakanishi, and T. Ando, *J. Phys. Soc. Jpn.* **68**, 716 (1999).
- <sup>12</sup>J.-C. Charlier, X. Blase, and S. Roche, *Rev. Mod. Phys.* **79**, 677 (2007).
- <sup>13</sup>A. V. Krasheninnikov and K. Nordlund, *J. Appl. Phys.* **107**, 071301 (2010).
- <sup>14</sup>S. Latil, S. Roche, D. Mayou, and J.-C. Charlier, *Phys. Rev. Lett.* **92**, 256805 (2004).
- <sup>15</sup>T. Ando, *J. Phys. Soc. Jpn.* **74**, 777 (2005).
- <sup>16</sup>H.-F. Song, J.-L. Zhu, and J.-J. Xiong, *Phys. Rev. B* **65**, 085408 (2002).
- <sup>17</sup>Y.-S. Lee, Marco Buongiorno Nardelli, and N. Marzari, *Phys. Rev. Lett.* **95**, 076804 (2005).
- <sup>18</sup>P. Partovi-Azar and A. Namiranian, *J. Phys. Condens. Matter* **20**, 135213 (2008).
- <sup>19</sup>A. Rochefort and P. Avouris, *J. Phys. Chem. A* **104**, 9807 (2000).
- <sup>20</sup>J. M. García-Lastra, K. S. Thygesen, M. Strange, and A. Rubio, *Phys. Rev. Lett.* **101**, 236806 (2008).
- <sup>21</sup>T. Vehviläinen, M. Ganchenkova, V. Borodin, and R. Nieminen, *J. Nanosci. Nanotech.* **9**, 4246 (2009).
- <sup>22</sup>Z. Zhang and K. Cho, *Phys. Rev. B* **75**, 075420 (2007).
- <sup>23</sup>M. Khazaei, M. S. Bahramy, A. Ranjbar, H. Mizuseki, and Y. Kawazoe, *Carbon* **47**, 3306 (2009).
- <sup>24</sup>M. Kim, N. S. Safron, E. Han, M. S. Arnold, and P. Gopalan, *Nano Lett.* **10**, 1125 (2010).
- <sup>25</sup>J. Bai, X. Zhong, S. Jiang, Y. Huang, and X. Duan, *Nature Nanotech.* **5**, 190 (2010).
- <sup>26</sup>J. A. Rodriguez-Manzo and F. Banhart, *Nano Lett.* **9**, 2285 (2009).
- <sup>27</sup>J. P. Perdew, K. Burke, and M. Ernzerhof, *Phys. Rev. Lett.* **77**, 3865 (1996).
- <sup>28</sup>J. M. Soler, E. Artacho, J. D. Gale, A. García, J. Junquera, P. Ordejón, and D. Sánchez-Portal, *J. Phys. Condens. Matter* **14**, 2745 (2002).
- <sup>29</sup>N. Troullier and J. L. Martins, *Phys. Rev. B* **43**, 1993 (1991).
- <sup>30</sup>M. Brandbyge, J.-L. Mozos, P. Ordejón, J. Taylor, and K. Stokbro, *Phys. Rev. B* **65**, 165401 (2002).
- <sup>31</sup>A. G. Nasibulin, P. V. Pikhitsa, H. Jiang, D. P. Brown, A. V. Krasheninnikov, A. S. Anisimov, P. Queipo, A. Moisala, D. Gonzalez, G. Lientschnig *et al.*, *Nature Nanotech.* **2**, 156 (2007).
- <sup>32</sup>J. A. Fürst, J. Hashemi, T. Markussen, M. Brandbyge, A. P. Jauho, and R. M. Nieminen, *Phys. Rev. B* **80**, 035427 (2009).